ACS MEASUREMENT SCIENCE Au
AN OPEN ACCESS JOURNAL OF THE AMERICAN CHEMICAL SOCIETY

pubs.acs.org/measureau
Article

Challenges in PFAS Postdegradation Analysis: Insights from the PFAS-CTAB Model System

Chanaka Navarathna,* Ransford Appianin Boateng, and Long Luo*

Cite This: ACS Meas. Sci. Au 2025, 5, 135−144
Read Online

ABSTRACT: Per- and polyfluoroalkyl substances (PFAS) are synthetic chemicals widely used for their oil and water-repellent properties. Their environmental persistence and potential health risks have raised significant concerns. As PFAS degrades through remediation or natural processes, they form complex mixtures of the original chemicals, transformation byproducts, and degradation additives. Analyzing PFAS after degradation presents analytical challenges due to possible chemical and physical interactions, including ion pairing, micelle formation, and complexation. These factors can significantly impact the precision and accuracy of PFAS measurements, yet they are often overlooked in PFAS degradation studies. In this work, we demonstrate that with the addition of ppb-level cetyltrimethylammonium bromide (CTAB), a cationic surfactant used in PFAS plasma-based degradation, the PFAS calibration curve linearity, sensitivity, and reproducibility are severely compromised. Isotopically labeled internal standards cannot fully correct these issues. Furthermore, the standard EPA methods 537.1, 533, and 1633 could not accurately recover PFAS concentrations in the PFAS and CTAB mixtures, with severe matrix effects observed for longer-chain and nitrogen-containing PFAS. Among these methods, Method 1633 is currently the most suitable option for postdegradation analysis. Method 1633 showed the lowest CTAB interference because this method used another weak ion pair additive, formic acid or acetic acid (in commercial lab analysis), to acidify the sample before LC−MS/MS analysis and added an isotopically labeled internal standard. For future PFAS degradation studies, we recommend systematically evaluating the matrix effect on the PFAS quantification using a recovery matrix to validate the analytical methods before use.

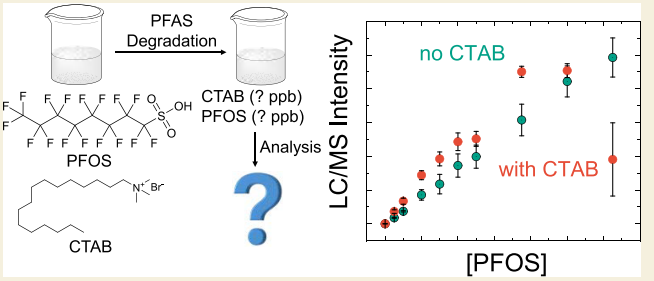

KEYWORDS: *PFAS, CTAB, degradation, analysis, LC−MS/MS*

1. INTRODUCTION

Per- and Polyfluoroalkyl Substances (PFAS) are a group of man-made chemicals widely used in industrial and consumer products since the 1940s due to their hydrophobicity, oleophobicity, and thermal/chemical stability.[1] These properties have made them popular for applications such as nonstick cookware, water-repellent clothing, stain-resistant fabrics and carpets, and firefighting foams. However, the characteristics that made PFAS valuable in these applications also make them persistent in the environment and human bodies as "forever chemicals".[2,3] Over the years, it became evident that PFAS causes potential health risks such as cancer, immuno suppression, and hormonal disruptions.[4−7] By the early 2000s, the environmental and health impacts of PFAS have gained significant attention, prompting regulatory actions and voluntary phase-out of certain PFAS compounds.[8]

The United States Environmental Protection Agency (EPA) has been working on addressing PFAS contamination through guidance, advisories, and regulation. In 2016, the EPA established a health advisory level for perfluorooctanoic acid (PFOA) and perfluorooctanesulfonate (PFOS) in drinking water at 70 parts per trillion (ppt) combined.[9] In 2023, the Biden-Harris administration proposed the first-ever national standard to regulate six PFAS in drinking water, marking a significant advancement in combating PFAS pollution.[10] The EPA has proposed maximum contaminant levels of 4 ppt for PFOA and PFOS, which is the current detection limit of interest for these compounds. For other PFAS such as PFNA, PFHxS, PFBS, and GenX, the EPA suggests using a hazard index to assess and regulate the cumulative risks from mixtures of these chemicals.[11]

The EPA has also developed a few standardized analytical methods, including 537.1,[12] 533,[13] and 1633,[14] for quantifying PFAS in different matrices. Method 537.1 is an update to the original Method 537 designed to determine the selected PFAS in drinking water. This method utilizes solid-phase extraction (SPE) and liquid chromatography-tandem mass spectrometry

Received: November 1, 2024
Revised: January 8, 2025
Accepted: January 9, 2025
Published: January 22, 2025

Table 1. Overview of Selected Representative PFAS Degradation Methods with Their Postdegradation PFAS Analysis Method

Degradation method	Potential interfering species	Solid-phase extraction (SPE)	Internal standards (IS)
Case1. CTAB-enhanced plasma degradation	CTAB	X	✓
Case 2. UV irradiation of 3-Indole-acetic-acid in 12-Aminolauric-modified montmorillonite	3-Indole-acetic-acid	X	X
Case 3. Micro-sulfidated zero-valent iron	Fe^{2+}/Fe^{3+}	N/A – Commercial lab analysis	
Case 4 - Zero-valent iron coupled with biochar		✓	✓

(LC−MS/MS) to identify and quantify 18 PFAS compounds, including both perfluoroalkyl carboxylic acids (PFCAs) and perfluoroalkyl sulfonic acids (PFSAs). Method 537.1 enhances the original method by improving detection limits and expanding the list of target PFAS. It is specifically tailored for treated and untreated drinking water but has also been used as a reference point for adapting methods for other matrices.[12,15] Method 533, complement to Method 537.1, focuses on a different set of PFAS compounds, primarily shorter-chain PFAS and their precursors. It also uses SPE and LC−MS/MS but targets 25 PFAS compounds, including 11 PFCAs, 12 PFSAs, and 2 GenX chemicals.[13] Method 533 uses isotope dilution and was developed in response to the evolving understanding of PFAS chemistry and toxicology, recognizing the need to monitor a broader array of compounds beyond those included in Method 537.1. Method 1633 represents a significant expansion in the scope of PFAS analysis by introducing various sample pretreatment approaches. It is designed to determine PFAS compounds in nonpotable water, solids, biosolids, and tissue samples. This method can analyze 40 PFAS compounds, including PFCAs, PFSAs, fluorotelomer alcohols, and other PFAS-related substances. Similar to the other two methods, Method 1633 uses SPE coupled with LC−MS/MS to achieve sensitive and accurate PFAS quantification in various environmental matrices.[14] The key differences in sample preparation and chromatographic conditions for these methods will be discussed later.

The scientific community, alongside the EPA, has dedicated significant efforts to PFAS analysis and degradation research over the past decade (Figure S1). Advanced PFAS degradation techniques, such as photocatalysis,[16,17] electrochemical oxidation/reduction,[18] plasma treatment,[19] and the use of potent chemical reductants such as zerovalent iron,[20−22] have shown promise in laboratory settings. These methods aim to break the C−F bonds, among the strongest in organic compounds, to degrade PFAS into less harmful substances. However, the postdegradation mixtures of PFAS consist of a complex array of compounds, including not only remaining PFAS but also their breakdown products such as F^- and sulfate, catalysts, electrolyte, and other additives such as indole, surfactants, and Fenton reagents.[22] The complexity of the postdegradation mixture poses a significant challenge in accurately quantifying the PFAS due to various possible interferences, which are not fully considered in the standard EPA methods. To address it, advanced analytical methods are also being developed for the quantification of PFAS in complex matrices based on matrix-assisted laser desorption/ionization mass spectrometry (MALDI−MS),[7] direct analysis in real-time mass spectrometry (DART−MS),[23] and ion mobility spectrometry.[24−26]

However, the PFAS postdegradation analysis in the literature has rarely followed the standard EPA methods and varied largely among different laboratories. Table S1 summarizes recent PFAS degradation methods in the literature, including their corresponding preconcentration, purification, and extraction techniques utilized before analysis, the mobile phases employed for LC−MS/MS, and the potential contaminants affecting analysis in the mixture after degradation. Table 1 selected a few examples. PFAS may form interactions through ion pairs, micelles, or complexation with the additives used in these cases. CTAB, being a cationic surfactant, can directly form ion pairs or micelles (Case 1).[19] Similarly, 3-indoleacetic acid can protonate in acidic medium, enabling ion-pair interactions with PFAS (Case 2).[27] Fe^{3+}/Fe^{2+} ions are known to form complexes with PFAS, which would affect the mass spectrometric analysis (Cases 3 and 4).[28] Cases 1[19] and 4[29] were performed with isotopically labeled internal standards, while Case 2[30] did not. Case 4 used SPE, while others did not. In Case 3,[31] information about the PFAS analysis was missing, as it was conducted at a commercial lab. Considering numerous studies have previously shown that simple adsorption onto LC−MS/MS vials and adherence to instrument components cause significant errors in PFAS analysis,[32,33] we wanted to find out the data reliability in the PFAS postdegradation analysis due to interference species from PFAS degradation and the variation of analytical procedures.

In this work, we focus on a model system containing a mixture of ppb-level cetyltrimethylammonium bromide (CTAB) and PFAS, which simulates a postdegradation mixture after CTAB-enhanced plasma-based PFAS destruction process.[19] We chose this model system because CTAB is known to form ion pairs with negatively charged PFAS,[34] which can change the retention times of PFAS compounds and affect the ionization efficiency for mass spectrometry quantification. We evaluated the PFAS quantification accuracy and reproducibility as a function of PFAS and CTAB concentrations. We observed that low concentration (5 to 125 ppb) of CTAB could severely compromise the PFAS calibration curve linearity, sensitivity, and reproducibility. The same irreproducible issue was observed even using the standard EPA methods 537.1, 533, and 1633. Adding isotopically labeled internal standards cannot fully correct these issues. We minimized CTAB interference by altering the mobile phase composition to 0.1% formic acid in water and acetonitrile mobile phase. Our results highlight the challenges in PFAS analysis in complex

https://doi.org/10.1021/acsmeasuresciau.4c00083
ACS Meas. Sci. Au 2025, 5, 135−144

postdegradation contexts, and the PFAS quantification method for analyzing postdegradation mixtures should be properly validated before use.

2. EXPERIMENTAL SECTION

2.1. Chemicals

Optima LC−MS grade (>99%) acetonitrile, methanol, and ultrapure water were purchased from Fischer Scientific. Ammonium acetate, formic acid (>99%), Perfluorooctanesulfonate (PFOS) and cetyltrimethylammonium bromide (CTAB) were purchased from Sigma-Aldrich. Perfluorohexanoic acid (PFHxA) sodium salt, Perfluoroheptanoic acid (PFHpA), Perfluorooctanoic acid (PFOA), Perfluorononanoic acid (PFNA), Perfluorodecanoic acid (PFDA), Perfluoroundecanoic acid (PFUA) sodium salt, Perfluorododecanoic acid (PFDoA), Perfluorotridecanoic acid (PFTrDA), Perfluorotetradecanoic acid (PFTeDA), Perfluorobutanesulfonate (PFBS) potassium salt, Potassium perfluorohexanesulfonate (PFHxS) (mixed isomers), Perfluorooctanesulfonate (PFOS) (mixed isomers), *N*-Methylperfluorooctanesulfonamidoacetic acid (*N*-MeFOSAA) (mixed isomers), *N*-Ethylperfluorooctanesulfonamidoacetic acid (*N*-EtFOSAA) (mixed isomers) and isotopically labeled sodium perfluoro-1-octanesulfonate (PFOS) ($^{13}C_8$, 99%), perfluoro-*n*-octanoic acid (PFOA) ($^{13}C_8$, 99%), potassium perfluoro-1-hexanesulfonate (PFHxS) ($^{13}C_6$, 99%) were purchased from Cambridge isotopes (item names: EF-28 native mix and ES-5648). The LC−MS/MS performance was validated using the IRMM-428 certified reference material, which includes Perfluorobutanesulfonate (PFBS), Perfluorohexanesulfonate (PFHxS), Linear perfluorooctanesulfonate (L-PFOS), Perfluoropentanoic acid (PFPeA), Perfluorohexanoic acid (PFHxA), and Perfluoroheptanoic acid (PFHpA).

2.2. Analytical Procedures

a. *LC−MS/MS configurations.* Two LC−MS/MS were mainly used in this study: one was a Shimadzu 8040 LC-Triple Quadrupole Mass Spectrometer equipped with an Electrospray Ionization source, and the other was an Agilent 6470B LC−MS/MS with an Agilent Jet Stream source. Analytical separation of PFAS and CTAB was achieved using a Waters ACQUITY UPLC BEH C18 column (130 Å, 1.7 μm, 2.1 mm × 100 mm), complemented by an Agilent InfinityLab Poroshell 120 guard column. A delay column, specifically the InfinityLab PFC Delay Column (4.6 × 30 mm) with a pressure tolerance of up to 1200 bar, was incorporated into the setup. PFAS are known for their tendency to stick to surfaces, including those in analytical instrumentation, which can lead to carry-over effects between samples or even contamination of the instrument itself, causing false-positive detections. PTFE tubing was substituted with PEEK tubing throughout the system to minimize potential cross-contamination.[35] Injection volumes were either 20 or 50 μL, with a 0.3 or 0.4 mL/min flow rate. The ESI capillary voltage was set to 2.5 kV, and the source temperature was set to 120 °C. The nebulizing gas flow rate was maintained at 3 L/min, the desolvation line temperature at 100 °C, the heat block temperature at 150 °C, and the drying gas flow rate at 15 L/min. The data loop time was set to 6 s. These parameters remained unchanged except when adjustments were necessary for standard methods. Multiple reaction monitoring mode was used in the analysis, and the MS/MS channel for each species was utilized for quantification. The MS/MS qualifiers and isolation windows are presented in Table S2. The PFAS sample preparation and LC gradients are given below.

b. *PFOS analysis.* An accelerated LC gradient was developed to analyze the PFOS-CTAB mixtures using a mobile phase of 20 mM ammonium acetate in water and methanol. Initially, the solvents were at 50% each, and methanol was ramped to 100% over 3 min, held at 100% for 2 min, then reduced back to 50%, and held for an additional 2 min. The total chromatography gradient duration was 7 min. The PFOS and CTAB concentrations ranged from 5 to 125 ppb. For internal standard experiments, 2.5 ppb of isotopically labeled PFOS was present in the samples. The same gradient program was used for the formic acid mobile phase experiments but with two mobile phase solutions being 0.1% formic acid in water and 0.1% formic acid in acetonitrile.

c. *PFAS mixture analysis.* The PFAS mixture samples were diluted from a Cambridge EPA 537 native mixture that contains PFHxA, PFHpA, PFOA, PFNA, PFDA, PFUA, PFDoA, PFTrDA, PFTeDA, PFBS, PFHxS, PFOS (each at 2 ppm), *N*-MeFOSAA and *N*-EtFOSAA (each at 8 ppm). The standard series was prepared in a concentration range of 5−125 ppb for each PFAS compound, with a fixed 100 ppb of isotopically labeled internal standard mixture of PFOS ($^{13}C_8$) and PFOA ($^{13}C_8$). The CTAB concentration was maintained at 2 ppm in the PFAS-CTAB mixture samples. The PFAS mixture samples were analyzed using the LC gradients in EPA methods 537, 1633, and a literature method that was previously used in the PFAS-CTAB plasma degradation study,[19] as well as by a commercial analytical laboratory, as specified below.

1. EPA Method 537.1. The gradient began with an initial mobile phase composition of 60% 20 mM ammonium acetate and 40% methanol, which was maintained for the first 1.0 min. From 1.0 to 25.0 min, the gradient increased the methanol percentage to 90% while decreasing ammonium acetate to 10%, and this composition was then held constant from 25.0 to 32.0 min. At 32.1 min, the gradient rapidly returned to the initial condition of 60% ammonium acetate and 40% methanol, which was maintained until 37.0 min to allow for re-equilibration of the column, preparing it for subsequent analyses.
2. EPA Method 1633. This method used a column temperature of 40 °C and a maximum pressure of 1100 bar. Before chromatography analysis, the sample pH was adjusted to 5.9−6.0 using formic acid and ammonium formate. The gradient started with 2% eluent A (acetonitrile) and 98% eluent B (2 mM ammonium acetate in 95:5 water/acetonitrile) at a flow rate of 0.35 mL/min, held from 0.0 to 0.2 min. By 4.0 min, the mixture changes to 30% eluent A and 70% eluent B with an increased flow rate of 0.40 mL/min. The composition shifted to 55% eluent A and 45% eluent B by 7.0 min, held until 9.0 min when eluent A reached 75%. At 10.0 min, eluent A reached 95% and then rapidly returned to 2% at 10.4 min, which was maintained until 11.8 min. The flow rate was reduced to 0.35 mL/min by 12.0 min for re-equilibration.
3. The literature method. The solvent gradient used eluent A (5 mM ammonium acetate in water) and eluent B (acetonitrile). It started at 0.4 mL/min with 20% eluent A and 80% eluent B, held from 0.0 to 0.5 min. By 3.0 min, the gradient shifted to 80% eluent A and 20% eluent B. At 5.0 min, eluent A was increased to 100%, which was held until 5.5 min. At 5.6 min, the gradient returned to the initial condition of 20% eluent A and 80% eluent B, maintained until 8.0 min for re-equilibration.
4. Commercial laboratory testing. The commercial sample analysis was conducted at Battelle following standard EPA 537.1, 533, and 1633 methods, using a Sciex 6500 (AD) LC−MS/MS. Low concentrations of PFAS (2 ppb for each PFAS except 8 ppb for *N*-MeFOSAA and *N*-EtFOSAA) and CTAB (24 ppb) were used because solid-phase extraction was used to preconcentrate the samples by 50−75 folds in these protocols. The commercial lab testing samples were stored and shipped in high-density polyethylene containers.
5. Quality control. A blank injection was performed between PFAS samples to ensure no carryover.

https://doi.org/10.1021/acsmeasuresciau.4c00083
ACS Meas. Sci. Au 2025, 5, 135−144

Chromatograms were monitored for residual PFAS and CTAB peaks. Injector needle wash was also performed with 50% H_2O and 50% MeOH before and after PFAS sample injection. Blank runs showing carryover residue peaks were repeated until the chromatograms returned to baseline. All samples were prepared in triplicate and injected twice during the analysis. The final average was calculated from six replicates, comprising both instrument and standard replicates.

3. RESULTS AND DISCUSSION

3.1. CTAB Interference on PFAS Quantification

3.1.1. Commercial Laboratory Analysis. In the original study of plasma degradation of PFAS by Li et al.,[19] the total PFAS concentration was ∼100 ppb, and the CTAB concentration was around 36.4 ppm (∼0.1 mM). Excess CTAB helped PFAS float to the liquid-foam interface, enabling the preconcentration of PFAS and facilitating plasma degradation. During plasma degradation, both CTAB and PFAS underwent decomposition. However, Li's original study did not determine the ratio of CTAB and PFAS in postdegradation mixtures (Figure 1a). To the first proximation,

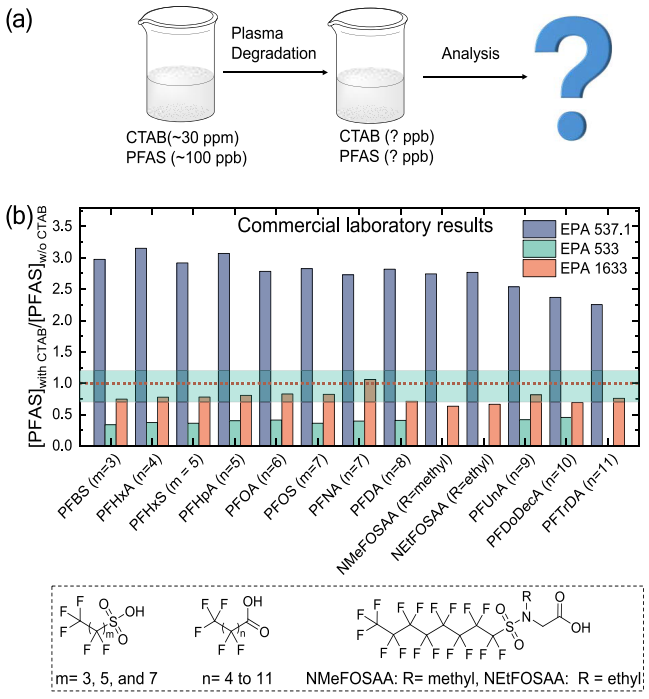

Figure 1. (a) Challenge in analyzing PFAS following plasma-degradation due to possible CTAB interference. (b) Ratio between PFAS concentrations with and without CTAB measured by a commercial laboratory using the standard EPA methods 537.1, 533, and 1633. PFAS samples contained 2 ppb of each PFAS except 8 ppb for NMeFOSAA and NEtFOSAA. Additional 24 ppb of CTAB was present in the CTAB-added PFAS mixture sample. Green zone highlights the $[PFAS]_{with\ CTAB}/[PFAS]_{w/o\ CTAB}$ ratio between 0.7 and 1.2.

we assumed the CTAB and PFAS left in the postdegradation mixture had comparable ppb-level concentrations.[19] Therefore, we prepared a PFAS mixture that contained 13 different PFAS compounds with equal concentrations of 2 ppb each, except for the two sulfonamide PFAS, NMeFOSAA and NEtFOSAA, which were 8 ppb each. The total PFAS concentration is 38 ppb. We spiked the PFAS mixture sample with 24 ppb CTAB to simulate the remaining CTAB in the degradation mixture.

Two PFAS mixture samples, one with CTAB and the other without CTAB, were submitted to a commercial analytical laboratory as blind samples to evaluate the CTAB interference on PFAS analysis. They were independently analyzed following the complete procedures of three different EPA methods 537.1,[12] 533,[13] and 1633,[14] which included solid-phase extraction, isotopically labeled internal standards, and surrogates. The main differences between the three EPA methods lie in sample preparation and chromatographic conditions. Briefly, Method 537.1 uses hydrophilic−lipophilic balanced SPE cartridges to extract PFAS, and its LC−MS/MS mobile phase consists of water and methanol with a relatively high concentration of ammonium acetate (20 mM). Method 533 utilizes mixed-mode SPE cartridges incorporating reversed-phase and weak anion exchange properties, allowing for better retention and extraction of short-chain PFAS and those in complex matrices. It uses a lower concentration of ammonium acetate (2 mM) in its LC−MS/MS mobile phase, aiming to optimize the detection of a broader array of PFAS. In contrast, Method 1633 uses a weak-anion exchange carbon SPE cartridge. Extracts were acidified with acetic acid, fortified with internal standards, and transferred to LC−MS/MS for analysis.

Surprisingly, none of the three methods produced satisfactory PFAS recovery for PFAS-only or PFAS-CTAB mixture samples (Table S3). For the PFAS-only sample, all reported PFAS concentrations were approximately ∼1/3 of the true concentrations for Method 533, ∼ 1/6 for Method 537.1, and ∼1/2 to 2/3 for Method 1633. We suspected such systematic underestimation most likely arises from SPE procedures. Because PFAS-only and PFAS-CTAB mixture samples were run in parallel in the commercial laboratory, similar systematic underestimation should be present for both samples. Thus, we focused on the ratio between the reported concentrations for PFAS-only or PFAS-CTAB mixture samples, which provides valuable information about the CTAB interference on PFAS analysis.

Figure 1b shows that Method 537.1 consistently reported ∼3 times higher PFAS concentrations in the presence of CTAB, while Method 533 reported only ∼1/3 of the PFAS concentration in the presence of CTAB. Among the three methods, EPA Method 1633 showed the smallest CTAB interferences with a concentration ratio ($[PFAS]_{with\ CTAB}/[PFAS]_{w/o\ CTAB}$) ranging from 0.65 to 1.11. The long-chain PFAS (PFDoDecA and PFTrDA) and sulfonamide PFAS (NMeFOSAA and NEtFOSAA) had relatively more significant interference than other PFAS. These results clearly show that CTAB strongly interferes with PFAS analysis, and EPA Method 1633 is currently the best choice for PFAS analysis in the presence of CTAB.

3.1.2. LC−MS/MS Analysis of CTAB and PFOS Mixtures. To understand the CTAB interference and find a potential solution, we started with a two-component model system of CTAB and PFOS mixtures with 0 to 125 ppb each. The simple composition allowed us to focus on the LC−MS/MS analysis without considering the sample extraction using SPE. We used the same mobile phase of ammonium acetate in water and methanol mixture as EPA Method 537.1 and modified chromatography conditions, as shown in Figure 2a, to accelerate the separation of PFOS and CTAB. Figure 2b shows the chromatogram acquired in the Multiple Reaction

https://doi.org/10.1021/acsmeasuresciau.4c00083
ACS Meas. Sci. Au 2025, 5, 135−144

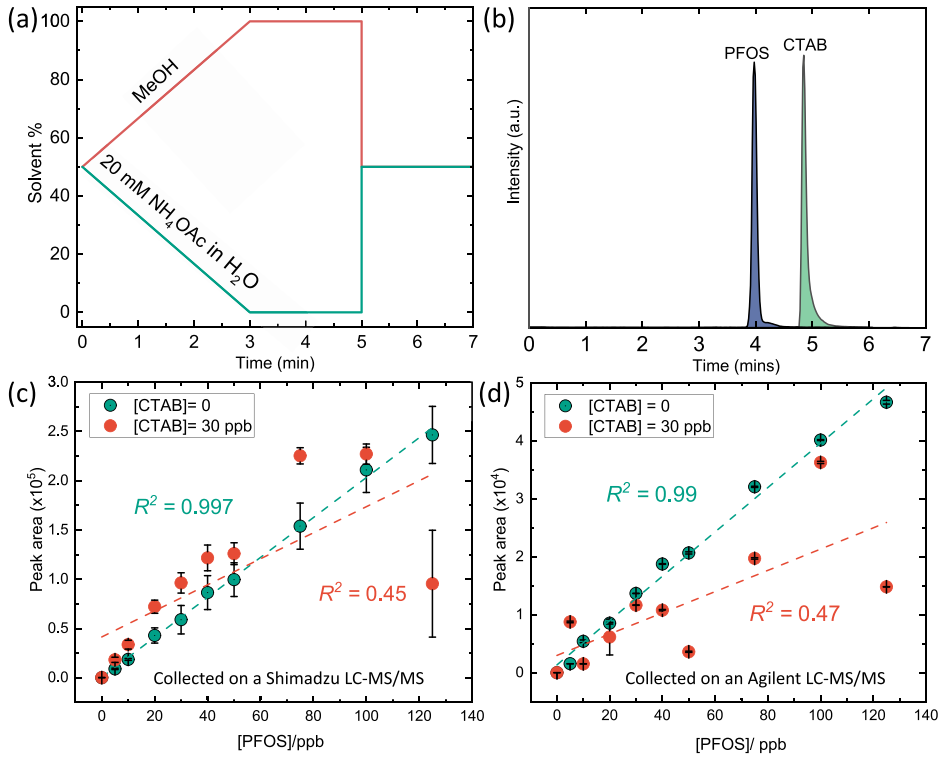

Figure 2. (a) Mobile phase gradient used for the accelerated LC−MS/MS analysis of PFOS and CTAB mixtures. (b) LC−MS/MS chromatogram for PFOS and CTAB acquired in multiple reactions monitoring mode. Flow rate: 0.3 mL/min. (c) PFOS calibration curves without CTAB and with [CTAB] = 30 ppb collected on a Shimadzu 8040 LC-Triple Quadrupole Mass Spectrometer at Wayne State University. (d) PFOS calibration curves collected on an Agilent 6470B LC−MS/MS at the University of Utah. Error bars represent the standard deviation of 3 replicates.

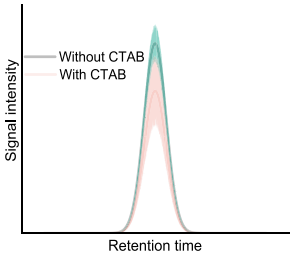

$$\text{Recovery} = \frac{\text{Peak area (with CTAB)}}{\text{Peak area (without CTAB)}}$$

(**Reproducibility**) = standard deviation of Recovery

<0.7	Poor
0.7-1.2	Good
>1.2	Poor

[CTAB]/ppb or nM		[PFOS]/ppb or nM								
		5	10	20	30	40	50	75	100	125
		0.01	0.03	0.05	0.08	0.11	0.14	0.21	0.27	0.34
0.25	125	1.79 (0.30)	1.63 (0.27)	1.09 (0.29)	1.42 (0.21)	1.60 (0.20)	1.52 (0.25)	1.01 (0.28)	1.00 (0.31)	1.01 (0.32)
0.2	100	1.4 (0.22)	1.33 (0.22)	1.83 (0.19)	1.17 (0.18)	1.23 (0.17)	1.26 (0.16)	1.37 (0.11)	0.88 (0.14)	1.13 (0.13)
0.15	75	1.04 (0.25)	1.07 (0.24)	0.86 (0.22)	1.06 (0.20)	1.50 (0.16)	0.38 (0.66)	1.2 (0.12)	0.92 (0.07)	0.92 (0.08)
0.1	50	0.76 (0.25)	0.82 (0.07)	0.83 (0.10)	0.78 (0.16)	1.21 (0.13)	1.30 (0.06)	1.05 (0.09)	1.02 (0.12)	1.06 (0.12)
0.08	40	1.66 (0.14)	1.47 (0.17)	1.04 (0.13)	1.13 (0.15)	0.94 (0.11)	1.20 (0.08)	1.23 (0.04)	1.22 (0.01)	1.30 (0.01)
0.06	30	2.03 (0.14)	1.80 (0.13)	1.68 (0.09)	1.63 (0.11)	1.41 (0.11)	1.26 (0.09)	1.46 (0.04)	1.08 (0.05)	0.39 (0.57)
0.04	20	2.32 (0.12)	2.03 (0.08)	0.40 (0.20)	1.69 (0.07)	1.51 (0.02)	1.04 (0.08)	0.38 (0.18)	1.24 (0.05)	1.29 (0.04)
0.03	10	2.15 (0.17)	1.84 (0.11)	1.54 (0.05)	1.58 (0.05)	1.43 (0.03)	1.57 (0.01)	1.45 (0.05)	1.35 (0.06)	1.39 (0.09)
0.01	5	0.99 (0.21)	0.96 (0.17)	0.98 (0.16)	1.15 (0.07)	1.34 (0.09)	1.24 (0.05)	1.20 (0.01)	1.24 (0.04)	1.04 (0.03)
0	0	1.00 (0.08)	1.00 (0.05)	1.00 (0.11)	1.00 (0.25)	1.00 (0.20)	1.00 (0.17)	1.00 (0.15)	1.00 (0.11)	1.00 (0.12)

Figure 3. Recovery matrix for PFOS analysis in the presence of 5 to 125 ppb CTAB. PFOS signal is averaged among three independent samples. Numbers in the parentheses are the standard deviations of the recovery values. Calibration curves used to generate this matrix are given in Figure S2.

Monitoring (MRM) mode for PFOS in the negative ion mode and CTAB in the positive ion mode. The LC−MS/MS analysis was performed on a Shimadzu 8040 LC-Triple Quadrupole Mass Spectrometer equipped with an electrospray ionization source at Wayne State University. Figure 2c shows that the calibration curve for PFAS has an R^2 of 0.997, with a stable slope and good reproducibility without CTAB. However, with the addition of just 30 ppb of CTAB, the curve began to lose

https://doi.org/10.1021/acsmeasuresciau.4c00083
ACS Meas. Sci. Au 2025, 5, 135−144

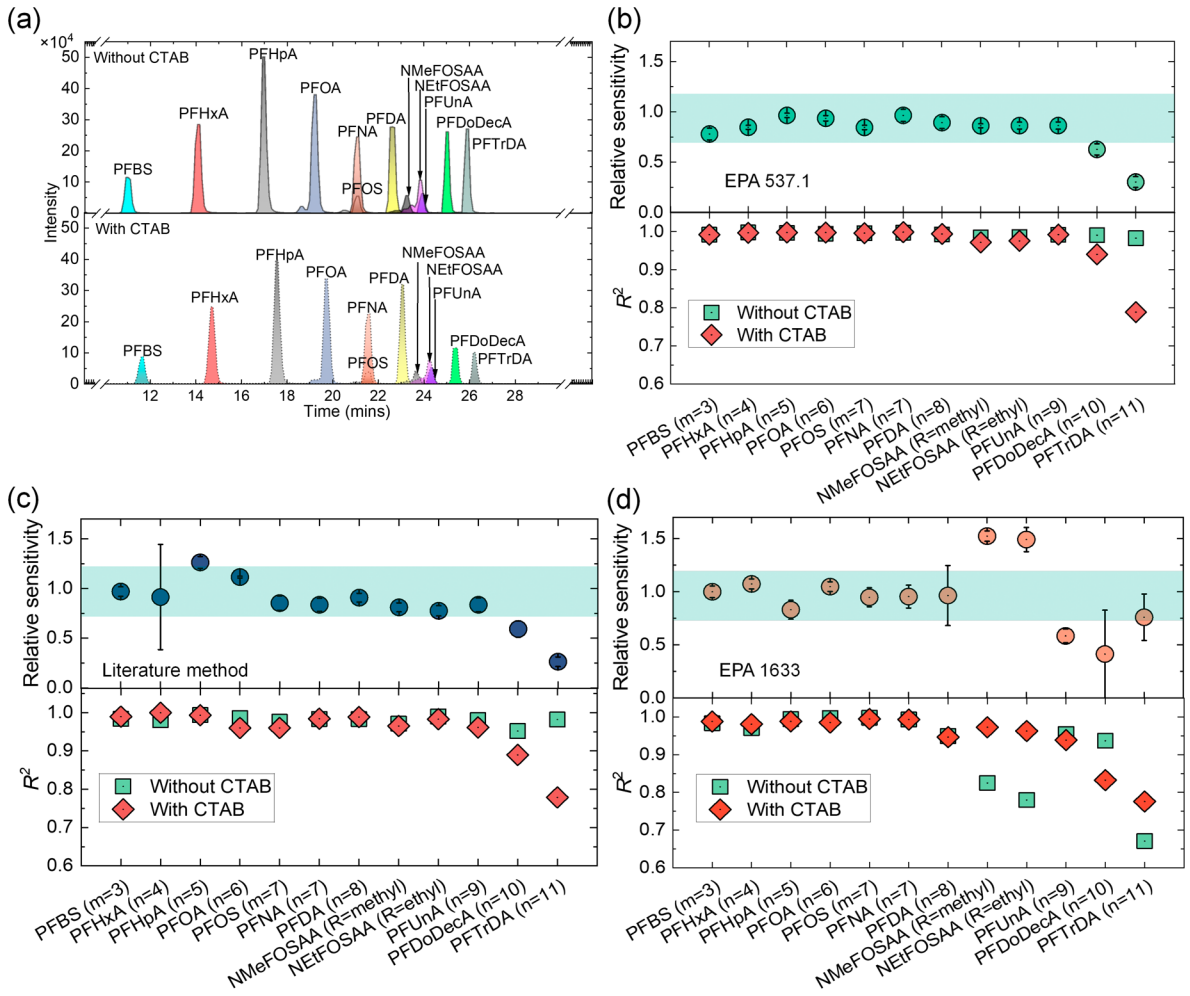

Figure 4. (a) Comparison between typical chromatograms for a PFAS mixture without and with CTAB using the EPA Method 537.1. Relative sensitivity and R^2 values for each PFAS compound in the mixture using the LC−MS/MS protocols in (b) EPA Method 537.1, (c) a previous literature method used in the PFAS-CTAB plasma degradation study,[19] and (d) EPA method 1633. Relative sensitivity is defined as the ratio between the slopes of the calibration curves for each PFAS with and without CTAB. Green shadow highlights the regions with a relative sensitivity of 0.7 to 1.2. Calibration curves used to calculate relative sensitivity and R^2 are provided in the Supporting Information, and error bars show the uncertainty of the relative sensitivity, calculated from the uncertainty of the linear fit slopes of the calibration curves with and without CTAB.

linearity with R^2 = 0.450. A similar change in calibration curve linearity and reproducibility was observed for other CTAB concentrations ≥20 ppb (Figure S2), confirming the strong interference of CTAB on the LC−MS/MS analysis.

To confirm that the observed interference from CTAB on PFOS analysis was not caused by instrument malfunctions, we performed the same analysis using an Agilent 6470B LC−MS/MS with an Agilent Jet Stream source at the University of Utah. We observed a similar linearity loss after adding CTAB (R^2 = 0.99 without CTAB vs R^2 = 0.47 without CTAB in Figure 2d).

We summarized the data collected on the Shimadzu 8040 LC−MS/MS for ten different CTAB concentrations ranging from 0 to 125 ppb in a PFOS recovery matrix (Figure 3). Each row in the matrix corresponds to a conventional calibration curve at a fixed CTAB concentration. Recovery is defined as the ratio between the LC−MS/MS signals of PFOS with and without CTAB to evaluate the CTAB interference, as expressed by eq 1.

$$\text{Recovery} = \frac{\text{PFOS signal with CTAB}}{\text{PFOS signal without CTAB}} \quad (1)$$

An acceptable recovery for analytical methods typically should be between 0.70 and 1.20 when no significant interference exists.[36] However, around 60% of the data points in the matrix fell outside this range (Figure 3). Most recovery values were over 1.2, with a maximum value of 2.32, indicating that CTAB tends to increase the LC−MS/MS signal. However, there are random cases where the recovery dropped to 0.38, suggesting the presence of CTAB can also cause a signal decrease. These random effects were not likely due to PFOS carryover, as blank runs were conducted before and after the PFOS analysis, and the signals for the blanks were comparable. No peaks corresponding to the presence of PFOS were observed (Figure S3). Inspection of the chromatographic profiles shows that CTAB and PFOS retention times remain mostly constant, with occasional early elution and tailing observed for PFOS (Figure S3). These early elutions could be attributed to PFOS-CTAB ion pairs or micelles that may exit the column without extensively partitioning into the analytical column.

3.1.3. LS−MS/MS Analysis of PFAS Mixtures. Next, we moved on to study the impact of CTAB on the LC−MS/MS analysis of standard PFAS mixtures. In this experiment, we

https://doi.org/10.1021/acsmeasuresciau.4c00083
ACS Meas. Sci. Au 2025, 5, 135−144

fixed the CTAB concentration at 2 ppm while varying the PFAS concentration from 5 to 125 ppb each, except for the two sulfonamide PFAS, NMeFOSAA and NEtFOSAA, which are 4 times high in concentration relative to other PFAS in the mixture. The maximum mass ratio between total PFAS and CTAB is ∼1, like the sample sent to the commercial laboratory. This time, we used three chromatographic conditions for PFAS analysis: EPA 537.1, EPA1633, and a previous literature method in the PFAS-CTAB plasma degradation study.[19] All three conditions achieved separation among different PFAS with similar reported retention times by EPA and PFAS-CTAB plasma degradation method (Figures 4a, S4, and Table S4).

For EPA Method 537.1, the peak position for each PFAS in the chromatogram did not show a significant shift after adding CTAB, but noticeable changes in the peak intensity were observed (Figure 4a). We established the calibration curves for each PFAS at various PFAS concentrations to evaluate the calibration curve linearity and signal sensitivity in the presence of CTAB (Figures S5−S10). We used relative sensitivity, defined as the ratio between the slopes of the calibration curves for each PFAS with and without CTAB, to evaluate the impact of CTAB on the PFAS signal. Figure 4b shows the relative sensitivity for most PFAS fell in the range of 0.7−1.2, except for the long-chain PFDoDecA and PFTrDA, which are as low as ∼0.3. Similarly, the linearity was maintained for most PFAS except PFDoDecA and PFTrDA. The latter two have a much worse R^2-value, as low as 0.78.

Similar results were observed using the literature method (Figure 4c),[19] which used ammonium acetate in acetonitrile and water as the mobile phase instead of methanol and water mixture in EPA 537.1. These findings indicate that CTAB mainly interacts with long-chain PFAS in a PFAS mixture in acetonitrile/water and methanol/water mobile phases, suppressing their mass spectrometric signals and causing irreproducible results.

Next, we tested the chromatographic condition of EPA Method 1633. This method was recently introduced to cover a broader sample scope, including aqueous, solid, biosolids, and tissue samples. The major difference between Method 1633 and the above two methods is that the sample pH was adjusted to 5−6 before chromatographic separation. The result in Figures 4d, S7, and S8 shows that (1) Method 1633 yielded poor linearity for two sulfonamide PFAS (NMeFOSAA and NEtFOSAA) and long-chain PFAS (PFTrDA) even without CTAB, (2) the presence of CTAB recovered the linearity for sulfonamide PFAS but increased the errors in each measurement (Figures S7 and S8), and (3) the linearity for two long-chain PFAS (PFDoDecA and PFTrDA) remained poor as other two methods. A possible explanation for the behaviors of sulfonamide PFAS is that their slightly higher pK_a values than other perfluorinated acids led to their protonation in an acidic medium and lowered the sensitivity.[37]

3.2. Origin of CTAB Interference and Potential Solutions

The LC−MS/MS studies above clearly show that CTAB strongly interferes with mass spectrometric analysis of PFAS, particularly for long-chain PFAS. This causes the poor linearity of the PFAS calibration curves in the presence of CTAB and, thus, inaccurate quantification.

3.2.1. Isotopically Labeled Internal Standards. Adding isotopically labeled internal standards is the most common strategy for addressing interference issues due to a complex matrix. We tested this strategy on the two-component CTAB-PFOS model system by adding $^{13}C_8$-labeled PFOS. Figure 5a shows that the LC−MS/MS calibration curve before adding CTAB has excellent linearity (R^2 = 0.990), but the R^2 value drops to 0.469, with the data points largely scattered after adding 30 ppb CTAB. After adding 2.5 ppb of $^{13}C_8$−PFOS as the internal standard, the calibration curve linearity for the PFOS-only sample was further improved with R^2 = 0.995 (Figure 5b). In comparison, the linearity was partially restored for the CTAB-PFOS mixture, but data remained scattered at the lower PFOS concentration region ([PFOS] ≤ 50 ppb), leading to a poor R^2 = 0.641. It is important to point out that the molar ratio of PFOS and CTAB at [PFOS] = 50 ppb and [CTAB] = 30 ppb is ∼1. This result suggests that when the PFOS/CTAB molar ratio in the sample is less than 1, $^{13}C_8$−PFOS also participates in the interactions with CTAB, causing irreproducible mass spectrometric signals. This finding also, in part, explained the CTAB interference observed in commercial laboratory testing results in Figure 1 even though isotopically labeled internal standards were used in the analysis (recall the total [PFAS] = 38 ppb and [CTAB] = 24 ppb, giving a PFAS/CTAB molar ratio = ∼ 1).

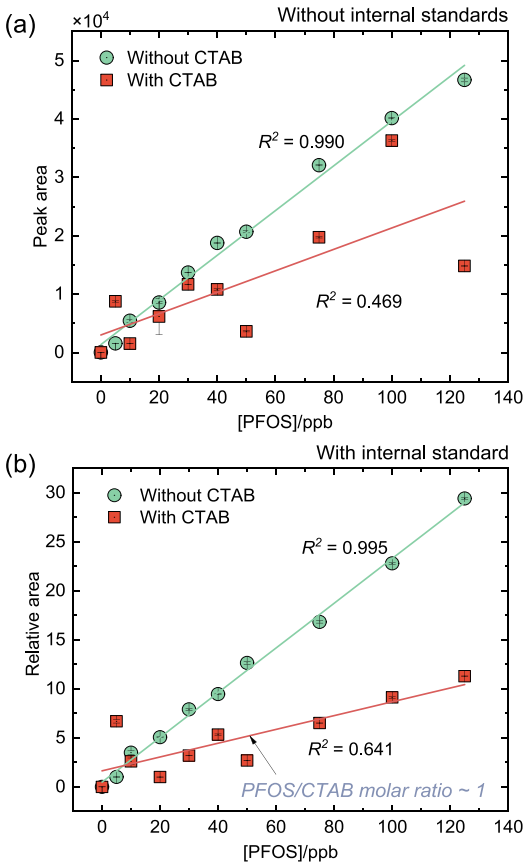

Figure 5. PFOS calibration curves with and without 30 ppb CTAB (a) in the absence of and (b) in the presence of 2.5 ppb $^{13}C_8$-labeled PFOS internal standard. Error bars represent the standard deviation of 3 replicates.

3.2.2. Formic Acid Mobile Phase. The dependence of the LC−MS/MS qualification accuracy on the PFOS/CTAB molar ratio suggests the presence of stoichiometric interactions between PFOS and CTAB, most likely the CTAB-PFOS ion pair formation. To mitigate the CTAB-PFOS ion pair

https://doi.org/10.1021/acsmeasuresciau.4c00083
ACS Meas. Sci. Au 2025, 5, 135−144

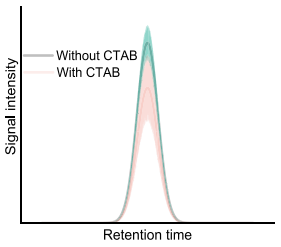

$$\text{Recovery} = \frac{\text{Peak area (with CTAB)}}{\text{Peak area (without CTAB)}}$$

$$(\textbf{Reproducibility}) = \text{standard deviation of Recovery}$$

<0.7	Poor
0.7-1.2	Good
>1.2	Poor

CTAB/ppb or nM		PFOS/ppb or nM: 5	10	20	30	40	50	75	100	125
		0.01	0.03	0.05	0.08	0.11	0.14	0.21	0.27	0.34
0.25	125	1.08 (0.19)	0.94 (0.06)	1.13 (0.09)	1.10 (0.01)	1.05 (0.01)	1.41 (0.01)	0.96 (0.00)	1.11 (0.27)	1.01 (0.14)
0.2	100	0.99 (0.02)	0.97 (0.05)	1.00 (0.00)	1.04 (0.01)	0.91 (0.01)	1.64 (0.00)	0.93 (0.00)	1.14 (0.02)	1.00 (0.03)
0.15	75	0.87 (0.02)	0.77 (0.02)	0.93 (0.01)	0.98 (0.01)	0.87 (0.02)	0.93 (0.02)	0.86 (0.02)	1.08 (0.02)	1.08 (0.02)
0.1	50	1.01 (0.01)	0.90 (0.03)	1.1 (0.00)	1.04 (0.01)	1.00 (0.01)	1.16 (0.01)	0.84 (0.01)	1.04 (0.02)	0.97 (0.03)
0.08	40	1.04 (0.02)	1.10 (0.02)	1.09 (0.00)	1.07 (0.01)	1.22 (0.01)	1.35 (0.01)	0.99 (0.01)	1.20 (0.04)	1.11 (0.03)
0.06	30	0.41 (0.11)	0.37 (0.01)	0.42 (0.01)	0.42 (0.00)	0.46 (0.01)	1.04 (0.01)	0.74 (0.00)	0.44 (0.09)	0.42 (0.01)
0.04	20	1.04 (0.06)	0.92 (0.04)	1.09 (0.01)	0.93 (0.01)	0.84 (0.01)	0.96 (0.01)	0.93 (0.00)	1.09 (0.05)	1.02 (0.01)
0.03	10	0.46 (0.01)	0.66 (0.02)	0.61 (0.01)	0.51 (0.01)	0.79 (0.01)	1.03 (0.01)	0.72 (0.01)	0.86 (0.03)	0.85 (0.05)
0.01	5	0.99 (0.04)	0.96 (0.01)	1.06 (0.02)	1.05 (0.01)	0.91 (0.01)	1.18 (0.01)	0.92 (0.01)	1.01 (0.08)	1.01 (0.02)
0	0	1.00 (0.01)	1.00 (0.02)	1.00 (0.01)	1.00 (0.02)	1.00 (0.01)	1.00 (0.00)	1.00 (0.01)	1.00 (0.01)	1.00 (0.01)

Figure 6. Recovery matrix for PFOS analysis in the presence of 5 to 125 ppb CTAB using 0.1% formic acid in water and acetonitrile as the LC−MS/MS mobile phase. Calibration curves used to generate this matrix are given in Figure S12.

formation effect, we adjusted the mobile phase from ammonium acetate in water and methanol (pH ∼ 8) to 0.1% formic acid in water and acetonitrile mixture (pH ∼ 3) (Figure S11). Formic acid is a weak ion-pairing agent that can also form ion pairs with CTAB,[38] which could suppress the formation of the CTAB-PFOS ion pair. Formic acid is also volatile and does not suppress the MS detector signal.[39,40] Figures 6 and S12 clearly show a significantly improved recovery, with the majority falling between 0.7 and 1.2 using this acidic mobile phase, even without internal standards. There were a few exceptions at [CTAB] = 10 and 30 ppb. The outlier data at 30 ppb was retested on an Agilent 6470B LC−MS/MS, but we observed similar inconsistent recovery. The reason is still unclear.

4. CONCLUSIONS

This study highlights the challenges in quantifying PFAS in the complex mixture after PFAS degradation using a simple PFAS-CTAB model system. The presence of CTAB significantly affects the LC−MS/MS signals of PFAS and the linearity of calibration curves for PFAS. The long PFAS compounds, such as PFDoDecA and PFTrDA, are more susceptible to CTAB interference than shorter ones in a PFAS mixture. Among the three standard EPA methods for PFAS analysis (Method 537.1, 533, and 1633), Method 1633 suffered the least from CTAB interference. The CTAB interference is most likely due to the ion pair formation with PFAS because the accuracy of the LC−MS/MS qualification depends on the PFOS/CTAB molar ratio. Using isotopically labeled internal standards could not fully address the interference issue and only improved the calibration curve linearity when the sample's PFOS/CTAB molar ratio was higher than 1. Using a mobile phase composed of formic acid in acetonitrile and water mixtures more effectively improved the quantification accuracy because formic acid is a weak pairing agent that can also form ion pairs with CTAB, which could suppress the formation of the CTAB-PFOS ion pair. Our findings are generally consistent with the commercial laboratory testing results that Method 1633 showed the lowest CTAB interference because this method used another weak ion pair reagent, acetic acid, to acidify the PFAS-CTAB mixture sample before LC−MS/MS analysis and added isotopically labeled internal standard. For future PFAS degradation studies, we recommend evaluating the matrix effect on the PFAS quantification using a recovery matrix to validate the analytical methods before use.

■ ASSOCIATED CONTENT

Supporting Information

The Supporting Information is available free of charge at https://pubs.acs.org/doi/10.1021/acsmeasuresciau.4c00083.

Publication information related to the analysis, degradation, and toxicity assessment of PFAS and calibration curves and chromatograms for outliers for PFOS, CTAB, and PFAS mixtures for standard methods, mass spectrometer collision energy, summary of selected representative methods for PFAS degradation/removal, LC−MS/MS analysis parameters, commercial laboratory PFAS analysis results, reported retention times for EPA 537.1, EPA 1633, and literature method (PDF)

■ AUTHOR INFORMATION

Corresponding Authors

Chanaka Navarathna − *Department of Chemistry, University of Utah, Salt Lake City, Utah 84112, United States*; Email: u6060400@utah.edu

Long Luo − *Department of Chemistry, University of Utah, Salt Lake City, Utah 84112, United States; Department of Chemistry, Wayne State University, Detroit, Michigan 48202, United States*; orcid.org/0000-0001-5771-6892; Email: long.luo@utah.edu

https://doi.org/10.1021/acsmeasuresciau.4c00083
ACS Meas. Sci. Au 2025, 5, 135−144

Author

Ransford Appianin Boateng − *Department of Chemistry, Wayne State University, Detroit, Michigan 48202, United States*

Complete contact information is available at: https://pubs.acs.org/10.1021/acsmeasuresciau.4c00083

Author Contributions

The manuscript was written with contributions from all authors. All authors have given approval to the final version of the manuscript. CRediT: L.L. conceptualization, data curation, methodology, resources, writing-review and editing; C.N. conceptualization, data curation, formal analysis, writing-review and editing; R.A.B. experimentation and formal analysis.

Notes

The authors declare no competing financial interest.

■ ACKNOWLEDGMENTS

This work is supported by the National Science Foundation under awards CHE-1943737 and CHE-2503459, the Department of the Army, United States Army Engineer Research and Development Center (ERDC), under Cooperative Agreement Number W912HZ2220002, the Alfred P. Sloan Foundation (Grant # FH-2023-20829), and the startup funds from the University of Utah.

■ REFERENCES

(1) Giesy, J. P.; Kannan, K. Perfluorochemical Surfactants in the Environment. *Environ. Sci. Technol.* **2002**, *36* (7), 146A−152A.

(2) Zareitalabad, P.; Siemens, J.; Hamer, M.; Amelung, W. Perfluorooctanoic acid (PFOA) and perfluorooctanesulfonic acid (PFOS) in surface waters, sediments, soils and wastewater−A review on concentrations and distribution coefficients. *Chemosphere* **2013**, *91* (6), 725−732.

(3) Baker, E. S.; Knappe, D. R. Per-and polyfluoroalkyl substances (PFAS)—contaminants of emerging concern. *Anal. Bioanal. Chem.* **2022**, *414* (3), 1187−1188.

(4) Sunderland, E. M.; Hu, X. C.; Dassuncao, C.; Tokranov, A. K.; Wagner, C. C.; Allen, J. G. A review of the pathways of human exposure to poly- and perfluoroalkyl substances (PFASs) and present understanding of health effects. *J. Expo. Sci. Environ. Epidemiol.* **2019**, *29* (2), 131−147.

(5) Savitz, D. A.; Stein, C. R.; Bartell, S. M.; Elston, B.; Gong, J.; Shin, H. M.; Wellenius, G. A. Perfluorooctanoic acid exposure and pregnancy outcome in a highly exposed community. *Epidemiology* **2012**, *23* (3), 386−392.

(6) Stahl, T.; Mattern, D.; Brunn, H. Toxicology of perfluorinated compounds. *Environ. Sci. Eur.* **2011**, *23* (1), 38.

(7) Reynolds, A. J.; Smith, A. M.; Qiu, T. A. Detection, Quantification, and Isomer Differentiation of Per- and Polyfluoroalkyl Substances (PFAS) Using MALDI-TOF with Trapped Ion Mobility. *J. Am. Soc. Mass Spectrom.* **2024**, *35* (2), 317−325.

(8) Cordner, A.; De La Rosa, V. Y.; Schaider, L. A.; Rudel, R. A.; Richter, L.; Brown, P. Guideline levels for PFOA and PFOS in drinking water: the role of scientific uncertainty, risk assessment decisions, and social factors. *Journal of exposure science & environmental epidemiology* **2019**, *29* (2), 157−171.

(9) U.S. EPA *Drinking Water Health Advisories for PFOA and PFOS.* https://www.epa.gov/ground-water-and-drinking-water/drinking-water-health-advisories-pfoa-and-pfos (accessed July 24, 2018).

(10) Watson, A. F. Remediation for PFAS Contamination: The Role of CERCLA Enforcement in Environmental Justice. *Ga. Law Rev.* **2024**, *58*, 803.

(11) Mumtaz, M.; Buser, M.; Pohl, H. Per-and polyfluoroalkyl mixtures toxicity assessment "Proof-of-Concept" illustration for the hazard index approach. *Journal of Toxicology and Environmental Health, Part A* **2021**, *84* (13), 553−567.

(12) Shoemaker, J. A.; Grimmett, P.; Boutin, B. *EPA Method 537. Determination of selected perfluorinated alkyl acids in drinking water by solid phase extraction and liquid chromatography/tandem mass spectrometry (LC/MS/MS)*; EPA, 2009.

(13) EPA *EPA Method 533: Determination of Per- and Polyfluoroalkyl Substances in Drinking Water by Isotope Dilution Anion Exchange Solid Phase Extraction and Liquid Chromatography/Tandem Mass Spectrometry*; EPA, 2019.

(14) EPA *Draft EPA Method 1633: Analysis of Per- and Polyfluoroalkyl Substances (PFAS) in Aqueous, Solid, Biosolids, and Tissue Samples by LC-MS/MS*; US EPA, 2021.

(15) Olomukoro, A. A.; DeRosa, C.; Gionfriddo, E. Investigation of the adsorption/desorption mechanism of perfluoroalkyl substances on HLB-WAX extraction phases for microextraction. *Anal. Chim. Acta* **2023**, *1260*, No. 341206.

(16) Cao, X.; Ding, L.; Peng, J.; Wang, W.; Zhang, Y.; Chang, Y.; Wang, T.; Soltan, W. B.; Cao, Z.; Liu, H. Efficient photocatalytic decomposition of PFOA over BiOI1-x with low power LED light. *Science of The Total Environment* **2024**, *951*, No. 175492.

(17) Hojamberdiev, M.; Larralde, A. L.; Vargas, R.; Madriz, L.; Yubuta, K.; Sannegowda, L. K.; Sadok, I.; Krzyszczak-Turczyn, A.; Oleszczuk, P.; Czech, B. Unlocking the effect of Zn 2+ on crystal structure, optical properties, and photocatalytic degradation of perfluoroalkyl substances (PFAS) of Bi 2 WO 6. *Environmental Science: Water Research & Technology* **2023**, *9* (11), 2866−2879.

(18) Calvillo Solís, J. J.; Sandoval-Pauker, C.; Bai, D.; Yin, S.; Senftle, T. P.; Villagrán, D. Electrochemical reduction of perfluorooctanoic acid (PFOA): an experimental and theoretical approach. *J. Am. Chem. Soc.* **2024**, *146* (15), 10687−10698.

(19) Li, R.; Isowamwen, O. F.; Ross, K. C.; Holsen, T. M.; Thagard, S. M. PFAS−CTAB complexation and its role on the removal of PFAS from a lab-prepared water and a reverse osmosis reject water using a plasma reactor. *Environ. Sci. Technol.* **2023**, *57* (34), 12901−12910.

(20) Fang, J.; Xu, K.; Liu, A.; Xue, Y.; Tie, L.; Deng, Z.; Qiu, R.; Zhang, W.-X. Selective perfluorooctanoic acid (PFOA) and perfluorooctane sulfonate (PFOS) adsorption by nanoscale zero-valent iron (nZVI): performance and mechanisms. *Environmental Science: Nano* **2024**, *11* (5), 1915−1925.

(21) Verma, S.; Lee, T.; Sahle-Demessie, E.; Ateia, M.; Nadagouda, M. N. Recent advances on PFAS degradation via thermal and nonthermal methods. *Chemical engineering journal advances* **2023**, *13*, No. 100421.

(22) Cui, J.; Gao, P.; Deng, Y. Destruction of Per- and Polyfluoroalkyl Substances (PFAS) with Advanced Reduction Processes (ARPs): A Critical Review. *Environ. Sci. Technol.* **2020**, *54* (7), 3752−3766.

(23) Emmons, R. V.; Fatigante, W.; Olomukoro, A. A.; Musselman, B.; Gionfriddo, E. Rapid Screening and Quantification of PFAS Enabled by SPME-DART-MS. *J. Am. Soc. Mass Spectrom.* **2023**, *34* (9), 1890−1897.

(24) Boatman, A. K.; Chappel, J. R.; Polera, M. E.; Dodds, J. N.; Belcher, S. M.; Baker, E. S. Assessing Per- and Polyfluoroalkyl Substances in Fish Fillet Using Non-Targeted Analyses. *Environ. Sci. Technol.* **2024**, *58* (32), 14486−14495.

(25) Dodds, J. N.; Kirkwood-Donelson, K. I.; Boatman, A. K.; Knappe, D. R. U.; Hall, N. S.; Schnetzer, A.; Baker, E. S. Evaluating Solid Phase Adsorption Toxin Tracking (SPATT) for passive monitoring of per- and polyfluoroalkyl substances (PFAS) with Ion Mobility Spectrometry-Mass Spectrometry (IMS-MS). *Science of The Total Environment* **2024**, *947*, No. 174574.

(26) Foster, M.; Rainey, M.; Watson, C.; Dodds, J. N.; Kirkwood, K. I.; Fernández, F. M.; Baker, E. S. Uncovering PFAS and Other Xenobiotics in the Dark Metabolome Using Ion Mobility Spectrometry, Mass Defect Analysis, and Machine Learning. *Environ. Sci. Technol.* **2022**, *56* (12), 9133−9143.

(27) Sheikhian, L.; Bina, S. Simultaneous extraction and HPLC determination of 3-indole butyric acid and 3-indole acetic acid in pea plant by using ionic liquid-modified silica as sorbent. *Journal of Chromatography B* **2016**, *1009*, 34−43.
(28) Rodrigo, P. M.; Navarathna, C.; Pham, M. T.; McClain, S. J.; Stokes, S.; Zhang, X.; Perez, F.; Gunatilake, S. R.; Karunanayake, A. G.; Anderson, R.; et al. Batch and fixed bed sorption of low to moderate concentrations of aqueous per-and poly-fluoroalkyl substances (PFAS) on Douglas fir biochar and its Fe3O4 hybrids. *Chemosphere* **2022**, *308*, No. 136155.
(29) Liu, Y.; Ptacek, C. J.; Baldwin, R. J.; Cooper, J. M.; Blowes, D. W. Application of zero-valent iron coupled with biochar for removal of perfluoroalkyl carboxylic and sulfonic acids from water under ambient environmental conditions. *Science of The Total Environment* **2020**, *719*, No. 137372.
(30) Kugler, A.; Dong, H. L.; Li, C.; Gu, C.; Schaefer, C. E.; Choi, Y. J.; Tran, D.; Spraul, M.; Higgins, C. P. Reductive defluorination of Perfluorooctanesulfonic acid (PFOS) by hydrated electrons generated upon UV irradiation of 3-Indole-acetic-acid in 12-Aminolauric-Modified montmorillonite. *Water Res.* **2021**, *200*, No. 117221.
(31) McGregor, R.; Zhao, Y. The in situ treatment of TCE and PFAS in groundwater within a silty sand aquifer. *Remediation* **2021**, *31* (2), 7−17.
(32) Mancini, M.; Gioia, V.; Simonetti, F.; Frugis, A.; Cinti, S. Evaluation of Pure PFAS Decrease in Controlled Settings. *ACS Meas Sci. Au* **2023**, *3* (6), 444−451.
(33) Zenobio, J. E.; Salawu, O. A.; Han, Z. W.; Adeleye, A. S. Adsorption of per- and polyfluoroalkyl substances (PFAS) to containers. *J. Hazard Mater. Adv.* **2022**, *7*, No. 100130.
(34) Brosseau, C. L.; Sheepwash, E.; Burgess, I. J.; Cholewa, E.; Roscoe, S. G.; Lipkowski, J. Adsorption of N-Decyl-N,N,N-trimethylammonium Triflate (DeTATf), a Cationic Surfactant, on the Au(111) Electrode Surface. *Langmuir* **2007**, *23* (4), 1784−1791.
(35) Bell, D. S. New Liquid Chromatography Columns and Accessories: What to Know for 2023. *LCGC Eur.* **2023**, *36* (05), 176−183.
(36) Schoenau, E. A. Elements of Method Design. In *Current Challenges and Advancements in Residue Analytical Methods*; American Chemical Society, 2019; Vol. *1300*, pp 3−16.
(37) Goss, K.-U. The pKa Values of PFOA and Other Highly Fluorinated Carboxylic Acids. *Environ. Sci. Technol.* **2008**, *42* (2), 456−458.
(38) You, J.; Wang, L.; Saji, M.; Olesik, S. V.; Ringel, M. D.; Lucas, D. M.; Byrd, J. C.; Freitas, M. A. High-sensitivity TFA-free LC-MS for profiling histones. *Proteomics* **2011**, *11* (16), 3326−3334.
(39) Núñez, O.; Lucci, P. Applications and uses of formic acid in liquid chromatography-mass spectrometry analysis. In *Advances in Chemistry Research*; Nova Science Publishers, 2013; Vol. *20*, pp 71−86.
(40) Nshanian, M.; Lakshmanan, R.; Chen, H.; Ogorzalek Loo, R. R.; Loo, J. A. Enhancing Sensitivity of Liquid Chromatography-Mass Spectrometry of Peptides and Proteins Using Supercharging Agents. *Int. J. Mass Spectrom.* **2018**, *427*, 157−164.

https://doi.org/10.1021/acsmeasuresciau.4c00083
ACS Meas. Sci. Au 2025, 5, 135−144